Coulomb screening and exciton binding energies in conjugated polymers

Eric Moore, Benjamin Gherman, and David Yaron
Department of Chemistry, Carnegie Mellon University, Pittsburgh, Pennsylvania 15213

(Received 15 October 1996; accepted 3 December 1996)

Hartree–Fock solutions of the Pariser–Parr–Pople and MNDO Hamiltonians are shown to give reasonable predictions for the ionization potentials and electron affinities of gas-phase polyenes. However, the energy predicted for formation of a free electron-hole pair on an isolated chain of polyacetylene is much larger than that seen in the solid state. The prediction is 6.2 eV if soliton formation is ignored and about 4.7 eV if soliton formation is included. The effects of interchain interactions on the exciton binding energy are then explored using a model system consisting of one solute and one solvent polyene, that are coplanar and separated by 4 Å. The lowering of the exciton binding energy is calculated by comparing the solvation energy of the exciton state to that of a single hole (a cationic solute polyene) and a single electron (an anionic solute polyene). It is argued that when the relative timescales of charge fluctuations on the solute and solvent chains are taken into account, it is difficult to rationalize the electron–electron screening implicit in the parametrization of a single-chain Hamiltonian to solid-state data. Instead, an electron–hole screening model is developed that includes the time scales of both the electron–hole motion and the solvent polarization. The predicted solvation energies, which are saturated with respect to solute and solvent chain length, are 0.07 eV for the exciton and 0.50 eV for a well separated electron–hole pair. Given this large, 0.43 eV reduction in the exciton binding energy due to interaction with a single chain, it seems likely that interchain interactions play a central role in establishing the solid-state exciton binding energy. [S0021-9606(97)50310-2]

I. INTRODUCTION

In light-emitting-diodes (LEDs) based on conjugated polymers, an electron and hole are injected into an undoped conjugated polymer, such as poly-(para-phenylene vinylene) (PPV).[1,2] These charges migrate through the material and combine to emit a photon. An important quantity for developing an understanding of this process is the exciton binding energy, the difference in energy between a well-separated electron–hole pair and the state that emits the photon. In polydiacetylene, both photoconductivity[3] and electroabsorption[4,5] measurements find an exciton binding energy of 0.5 eV. In polyacetylene, photoexcitation leads to the rapid formation of both charged and neutral solitons.[6–8] In PPV, experimental estimates for the exciton binding energy include near 0.0,[9] 0.2 eV,[10] 0.4 eV,[11,12] and 0.9 eV,[13,14] and theoretical estimates include 0.4 eV (Ref. 15, 16) and 0.9 eV.[14]

Here, we use semiempirical quantum chemistry to predict the exciton binding energy of an isolated polymer chain, and to explore the effects of interchain interactions on this binding energy. Many theoretical studies of conjugated polymers use a single-chain Hamiltonian with parameters fit to solid-state observations.[14,17–20] The resulting parameters are typically quite different from those used in standard semiempirical quantum chemistry models such as PPP,[21] ZINDO,[22] or MNDO.[23] In particular, to obtain agreement with solid-state exciton binding energies, the Coulomb repulsion between electrons must be substantially weaker than that present in standard chemical parametrizations.[17,19,14] This need to weaken the electron–electron interactions in a single-chain Hamiltonian may reflect the importance of Coulomb screening from adjacent polymer chains. Our goal is to develop explicit models for this screening process. Explicit inclusion of screening will likely lead to better transferability of parameters between different polymer systems. It should also allow detailed information on molecules, either from experiment or high-level *ab initio* calculations, to be used in the parametrization of solid-state models. The use of molecular data is especially important when detailed solid-state experimental data are difficult to obtain, such as when modeling the effects of chemical defects and physical morphology.

The effects of interchain interactions on the exciton binding energy are studied using a model system consisting of one ''solute'' polyene and one ''solvent'' polyene.[24,25] When the relative time scales of charge fluctuations on the solute and solvent chains are taken into account, it is difficult to rationalize the electron–electron screening implicit in the parametrization of a single-chain Hamiltonian to solid-state data. Instead, we adopt an electron–hole screening model and demonstrate that the relative time scales of electron–hole motion and solvent polarization are such that a simple screening of the electron–hole interaction is not valid.

Section II describes the chemical system being studied and defines the Hamiltonian. Section III uses semiempirical quantum chemistry to extrapolate the ionization potential and electron affinity of polyenes[26] to the long chain limit, yielding a prediction for the energy required to create a free electron–hole pair on an isolated polyacetylene chain. Section IV develops models for the effects of interchain interactions on the exciton binding energy, Sec. IV A introduces the quantum chemical basis set used to describe the polarization of the solvent chain, Sec. IV B discusses the time scales of importance to the screening process, Secs. IV C and IV D

 0021-9606/97/106(10)/4216/12/$10.00

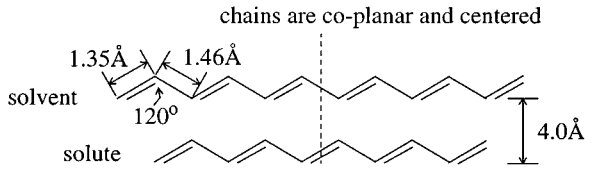

FIG. 1. Chemical structure of the system used to study the effects of interchain interactions on the exciton binding energy. Both the solute and solvent chain lengths are varied in the calculations.

consider simple limiting cases for these time scales, and Sec. IV E develops a general electron–hole screening model that includes the time scales of both electron–hole motion and the dielectric response. The results of these models are compared and discussed in Sec. V.

II. HAMILTONIAN

The solvation energy calculations are performed on a model system consisting of two polyenes, one solute and one solvent chain (Fig. 1). The Hamiltonian is,

$$H = H^{\mathrm{sol}} + H^{\mathrm{solv}} + H^{\mathrm{sol-solv}}. \tag{1}$$

The solute is described using Pariser–Parr–Pople theory,[21]

$$H^{\mathrm{sol}} = \sum_{i,j,\sigma} [-I\delta_{i,j} + \alpha^{\mathrm{sol}}_{j,i}] a^{\dagger}_{j,\sigma} a_{i,\sigma} + \frac{1}{2}\sum_{i} U(\hat{\rho}_i - 1)\hat{\rho}_i + \sum_{i<j} U(r_{j,i})\hat{\rho}_j\hat{\rho}_i, \tag{2}$$

where $a^{\dagger}_{i,\sigma}(a_{i,\sigma})$ creates (destroys) an electron with spin σ in the p-orbital on the ith carbon, $\hat{\rho}_i$ is the charge operator on the ith carbon, $\hat{\rho}_i = 1 - a^{\dagger}_{i,\alpha}a_{i,\alpha} - a^{\dagger}_{i,\beta}a_{i,\beta}$, and $r_{i,j}$ is the distance between carbons i and j. For the one electron terms, $\alpha^{\mathrm{sol}}_{j,i}$, we use nearest-neighbor transfer integrals of $\beta^{\mathrm{sol}}_1 = -2.228$ eV for single bonds and $\beta^{\mathrm{sol}}_2 = -2.581$ eV for double bonds. Both the electron–electron and nuclear–nuclear repulsions are described with the Ohno potential,

$$U(r) = \frac{14.397 \ \text{eV A}}{\sqrt{\left(\frac{14.397 \ \text{eV A}}{U}\right)^2 + r^2}}, \tag{3}$$

where U is the Hubbard parameter. I and U are chosen such that application of the Hamiltonian to a single carbon atom yields the ionization potential and electron affinity of an sp^2 hybridized carbon; I is set equal to the ionization potential of an sp^2 hybridized carbon, 11.16 eV, and U is set equal to the difference between the ionization potential and electron affinity of an sp^2 hybridized carbon, $U = 11.13$ eV.[27]

The solvent is described using Hückel theory,

$$H^{\mathrm{solv}} = \sum_{I,J,\sigma} \alpha^{\mathrm{solv}}_{J,I} a^{\dagger}_{J,\sigma} a_{I,\sigma}, \tag{4}$$

with $\alpha^{\mathrm{solv}}_{J,I}$ being nearest-neighbor transfer integrals chosen such that $(\beta^{\mathrm{solv}}_1 + \beta^{\mathrm{solv}}_2)/2 = -2.4045$ eV, as in the PPP model, and

$$|\beta^{\mathrm{solv}}_1 - \beta^{\mathrm{solv}}_2| = E^{\mathrm{solv}}_g/2, \tag{5}$$

where E^{solv}_g is the optical gap of the solvent (1.8 eV in all studies except those of Fig. 12). Hückel theory is used for the solvent because it greatly simplifies the Hamiltonian matrix elements in the electronic–polaron model of Sec. IV E (see the Appendix), and because it should provide a reasonable description of the linear response of the solvent chain. Unlike dielectric continuum models, which implicitly assume a solvent made up of point dipoles, Hückel theory captures the delocalized electronic structure of the solvent. Hückel theory also contains the correct time scale for the dielectric response, an issue of importance in the electronic–polaron model of Sec. IV E. This time scale is set by the optical gap and the Hückel parameters are chosen to yield the experimentally observed optical gap, Eq. (5).

The solute and solvent interact through Coulomb interactions,

$$H^{\mathrm{sol-solv}} = \sum_{I,i} U(r_{I,i})\hat{\rho}_I\hat{\rho}_i, \tag{6}$$

where i is summed over solute atoms and I is summed over solvent atoms.

III. EXCITON BINDING ENERGY ON AN ISOLATED POLYMER CHAIN

It is useful to separate the calculation of the exciton binding energy into two parts; the exciton binding energy of a hypothetical isolated chain, and the effects of interchain interactions on this binding energy. This section first calculates the exciton binding energy of a single polyacetylene chain using the PPP Hamiltonian and S-CI (configuration interaction with single electron–hole pair excitations) theory,[28–30,17–19] since this is the approach that is used to describe the solute in Sec. IV. We then consider semiempirical models that include both sigma and pi electrons. These allow us to compare the theoretical predictions to experiments on carbon chains with both even and odd numbers of carbon atoms, and to include the soliton formation energy.

In Sec. IV, the PPP Hamiltonian for the solute chain, Eq. (2), is solved using S-CI theory in a local orbital basis. The local orbitals are obtained from the canonical Hartree–Fock orbitals using the localization method of Ohmine *et al.*,[21] and consist of one occupied ''valence-band'' orbital and one unoccupied ''conduction-band'' orbital centered on each unit cell, or carbon–carbon double bond. In S-CI theory,[28] the ground state remains the Hartree–Fock ground state and the excited states are determined variationally using the trial form,

$$\Psi^{\text{isolated neutral}} = \sum_{a,r} c^r_a \psi^r_a, \tag{7}$$

where ψ^r_a has a hole in the valence-band orbital centered on the ath unit cell and an electron in the conduction-band orbital centered on the rth unit cell. The summation is over all positions of the electron and hole. With the parameters of

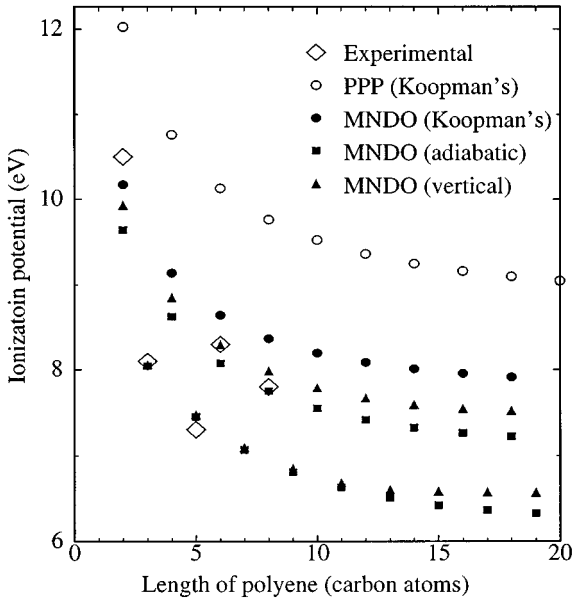

FIG. 2. Ionization potentials of polyenes, $C_{2n}H_{2n+2}$, calculated using the PPP and MNDO Hamiltonians (Ref. 35). Koopman's theorem results are shown, along with results obtained by comparing the Hartree–Fock energies of the neutrals and ions. Experimental values are from Ref. 26.

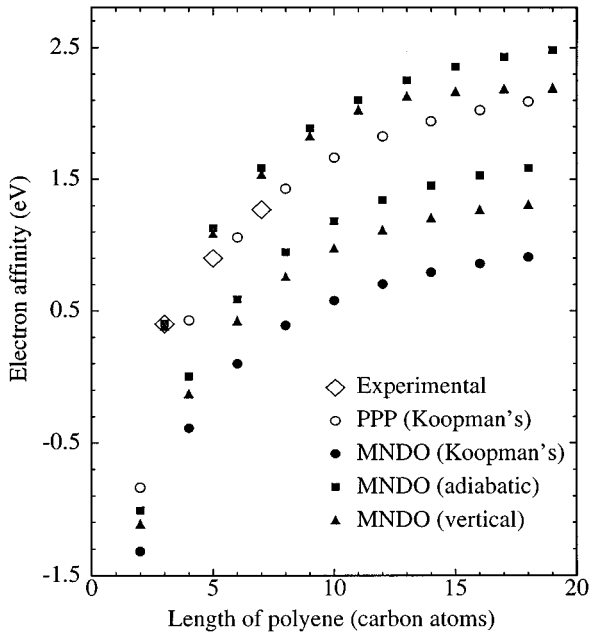

FIG. 3. Electron affinities of polyenes, $C_{2n}H_{2n+2}$, calculated as in Fig. 2. Due to the minimal basis nature of the calculation, negative values for the electron affinity are obtained for small polyenes. These negative values are shown only to illustrate the chain-length dependence of the calculated electron affinity. Experimental values are from Ref. 26.

Sec. II, the $1\,^1B_u$ optical gap state contains a tightly-bound electron–hole pair, and free electron–hole pair states begin at the Hartree–Fock band gap.[30,18]

Rather than use S-CI theory to generate free electron–hole pair states, we consider a single hole (a cationic polyene) and a single electron (an anionic polyene). The cationic polyene is described with the variational trial form,

$$\Psi^{\text{isolated cation}}=\sum_a c_a\psi_a, \tag{8}$$

where ψ_a has a hole in the valence-band orbital centered on the ath unit cell. An analogous form is used for the anion. Using Eq. (8), the energy of the cation relative to that of the neutral polyene is given by the energy of the highest-occupied-molecular-orbital (HOMO); thus this procedure yields the Koopman's theorem ionization potential (IP).[28] Similarly, the anion's energy is given by that of the lowest-unoccupied-molecular-orbital (LUMO), and this procedure yields the Koopman's theorem electron affinity (EA). The energy required to create a free electron–hole pair on a long chain is then taken as the polymeric limit of IP–EA. The resulting IP–EA is the difference between the Hartree–Fock HOMO and LUMO orbital energies. This approach is thus equivalent to S-CI theory in the long-chain limit, where free electron–hole pair states begin at the Hartree–Fock band gap.

The PPP Koopman's theorem IP's and EA's are shown in Figs. 2 and 3. The long-chain limit of IP–EA is about 6.9 eV. Since the $1\,^1B_u$ optical gap obtained from S-CI theory is 2.5 eV,[30,31] this corresponds to an exciton binding energy of about 4.4 eV. Note that the exciton binding energy is set primarily by the electron–electron interaction potential, $U(r)$ of Eq. (3). [While I of Eq. (2) displaces the calculated IP and EA, it has no effect on either the predicted $1\,^1B_u$ optical gap or on IP–EA.] The Ohno potential value for U, 11.13 eV, is based on the ionization potential and electron affinity of an sp^2 hybridized carbon.[27] This is not unique to pi electron theory. Other semiempirical Hamiltonians, such as ZINDO,[22] MNDO,[23] and AM1,[32] also use properties of the isolated atoms to parametrize the electron–electron interactions. It is worth noting that the Ohno potential gives reasonable agreement with the experimental energy of the $2\,^1A_g$ state of polyenes, a quantity that is very sensitive to the strength of electron–electron interactions.[21,33,34]

To allow comparison with experimental IP's and EA's of polyenes with both even and odd numbers of carbon atoms, and to allow inclusion of soliton formation energies, we also consider MNDO (Ref. 23) calculations in Figs. 2–4.[35] The MNDO Koopman's theorem IP–EA is about 7.0 eV, similar to the 6.9 eV of PPP theory. The points labeled vertical IP and EA refer to calculations in which the Hartree–Fock orbitals of the cation and anion are allowed to relax after addition or removal of the electron. Orbital relaxation lowers IP–EA of chains with an even number of carbon atoms to about 6.2 eV. Inclusion of geometric relaxation in the cation and anion, as in the adiabatic IP and EA of Figs. 2 and 3, lowers IP–EA of even carbon chains to 5.6 eV.

In the calculations of Fig. 4, the soliton formation energy is included by considering the process

$$2C_{2n}H_{2n+2}\rightarrow C_{2n-1}H_{2n+1}{}^{+1}+C_{2n+1}H_{2n+3}{}^{-1}, \tag{9}$$

where n is an integer and the molecules are noninteracting. Charged chains with an odd number of carbon atoms are

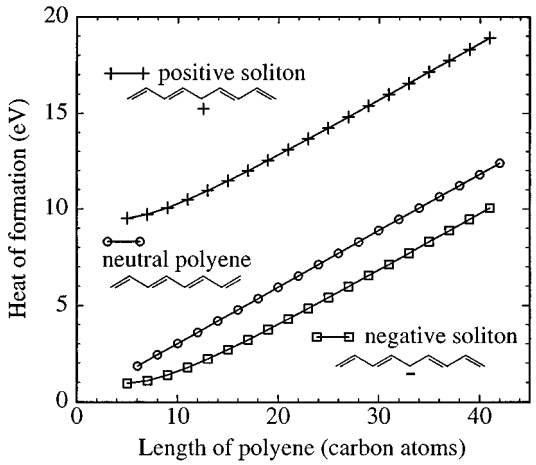

FIG. 4. Heats of formation of polyenes, $C_{2n}H_{2n+2}$, obtained using the MNDO Hamiltonian (Ref. 35). The charged polyenes shown here have an odd number of carbon atoms, since these can support a single charged soliton. As discussed below Eq. (9), comparison of these results yields a prediction of 4.7 eV for the energy required to create a well-separated positive and negative soliton on an isolated chain of polyacetylene.

used since such chains can support a single charged soliton. In the long chain limit, $n\rightarrow\infty$, the energy of the above reaction is equal to the energy required to create a well-separated positive and negative soliton on a single chain, 4.7 eV for the MNDO results of Fig. 4. Similar results are obtained with the MINDO (4.4 eV), AM1 (4.5 eV) and PM3 (4.7 eV) Hamiltonians.[35] This is much larger than the observed threshold for charged soliton production in polyacetylene, which is very near the optical gap of around 1.8 eV.[6–8]

Similar results are obtained from S-CI theory on other polymers and using other semiempirical Hamiltonians. For instance in PPV, S-CI solution of the PPP Hamiltonian with Ohno parameterization yields an exciton binding energy of about 3 eV,[14] and S-CI/INDO calculations yield an exciton binding energy of about 2.75 eV.[36]

Since semiempirical calculations that include orbital relaxation give good agreement with the ionization potential and electron affinity of short polyenes,[26] the calculations of Figs. 2–4 may be viewed as using semiempirical Hartree–Fock theory to extrapolate from experimental results on short polyenes to the long-chain limit. There is a potential problem with this extrapolation procedure. Suhai[37,38] and Liegener[39] find that when dynamic correlation is included in single-chain calculations, an on-chain polarization cloud is formed around the charges and this significantly lowers the exciton binding energy. This effect of dynamic correlation may become increasingly important on longer chains, and its absence from the calculations of Figs. 2–4 may mean that the long-chain limits of IP and EA are not reliable. We comment on this further in Sec. V. The remainder of this paper focuses on another factor that likely plays a central role in establishing the exciton binding energy—dielectric interactions between chains.

IV. EFFECT OF INTERCHAIN INTERACTIONS

Dielectric interactions with surrounding chains lower the exciton binding energy because the solvation energy of the free electron–hole pair is greater than that of the exciton. The calculations presented here compare the solvation energy of a single electron (a polyene anion) and hole (a polyene cation) to that of the exciton. Due to particle–hole symmetry in Eq. (1), the solvation energy of the anion is equal to that of the cation, and only that of the cation is reported below.

A. Description of solvent polarization

The polarization induced in the solvent by a *static* charge distribution on the solute is obtained from the following Hamiltonian:

$$H' = H^{\mathrm{solv}} + \sum_{I,i} \Gamma_{I,i} \hat{\rho}_I \langle \hat{\rho}_i \rangle, \tag{10}$$

where H^{solv} is the Hückel Hamiltonian of Eq. (4), and the second term is similar to Eq. (6) but with $\langle \hat{\rho}_i \rangle$ the static charge on the i^{th} solute atom. The solvation energy is the difference in energy between the ground state of the isolated solvent chain, as described by H^{solv}, and the ground state of H'.

To describe the polarization induced by a dynamic solute charge distribution, the electronic–polaron model of Sec. IV E uses a basis set for the solvent polarization. Here, we introduce this basis and test it by calculating the solvation energy of various static charge distributions.

The solvent basis functions are Φ_0, the unpolarized solvent, and Φ_a and Φ_a^r, the solvent as polarized by various positions of the electron and hole on the solute. Φ_0 is the ground state of the isolated solvent, as described by H^{solv} of Eq. (4). Φ_a is the ground state of the solvent in the presence of a hole on the ath unit cell of the solute. More precisely, Φ_a is the ground state of H' in Eq. (10), with $\langle \hat{\rho}_i \rangle = \zeta \langle \psi_a | \hat{\rho}_i | \psi_a \rangle$, where ψ_a is the wave function of a solute with a hole on the ath unit cell, see Eq. (8). The magnitude of the solute charge distribution is multiplied by a constant scaling factor, ζ, for reasons to be discussed below. Φ_a^r is the polarization induced in the solvent by a hole on the ath unit cell and an electron on the rth unit cell of the solute. More precisely, Φ_a^r is the ground state of H' in Eq. (10), with $\langle \hat{\rho}_i \rangle = \zeta \langle \psi_a^r | \hat{\rho}_i | \psi_a^r \rangle$, where ψ_a^r is the solute wave function of Eq. (7). When calculating the polarization induced by a polyene cation, the solvent basis set is,

$$\Psi^{\mathrm{solvent}} = c_0 \Phi_0 + \sum_{a=1}^{N} c_a \Phi_a, \tag{11}$$

where N is the number of unit cells on the solute. When calculating the polarization induced by the exciton state, the solvent basis set is,

$$\Psi^{\mathrm{solvent}} = c_0 \Phi_0 + \sum_{a,r=1}^{N} c_a^r \Phi_a^r. \tag{12}$$

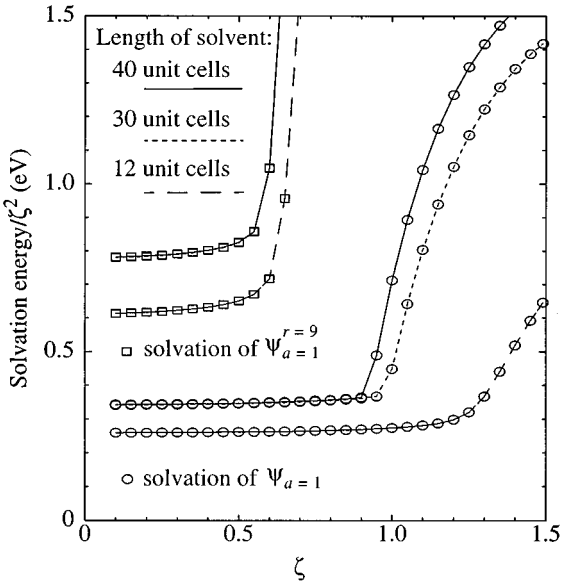

FIG. 5. Solvation energy of static charge distributions calculated by direct solution of the Hamiltonian in Eq. (10). Results labeled $\psi_{a=1}$ are for the charge distribution arising from a hole on the first unit cell of a solute with 9 unit cells. $\psi_{a=1}^{r=9}$ refers to a hole on the first unit cell and an electron on the 9th unit cell of a solute with 9 unit cells. The charge distributions are multiplied by a scaling factor, ζ. For a linear solvent response, the solvation energy should be proportional to ζ^2. The rapid increase beyond a critical value of ζ is due to the formation of a charge-separated ground state on the solvent chain.

Note that the solvent basis functions, Φ_0, Φ_a, and Φ_a^r are normalized but not orthogonal.

The basis sets of Eqs. (11) and (12) will be used to describe the polarization induced by an exciton or a hole delocalized over a polymer. These charge distributions are much more diffuse than the charge distributions of ψ_a or ψ_a^r, which describe holes and electrons localized at specific positions on the solute. Thus in generating Φ_a and Φ_a^r, the solute charge distribution is multiplied by the scaling parameter, $\zeta<1$. This is also useful because the localized charge distributions of ψ_a or ψ_a^r can induce charge separation in the solvent. We will show below that the basis set performs best when ζ is chosen such that Φ_a and Φ_a^r are not in the charge-separated regime.

The circles in Fig. 5 show the solvation energy of the charge distribution corresponding to a hole on the first unit cell of a 9 unit cell solute, multiplied by the scaling factor ζ. For a linear solvent response, the solvation energy is proportional to ζ^2, and it is this proportionality constant that is shown in the figure. The response is approximately linear for scaling factors, ζ, below some critical value, beyond which the solvation energy becomes large and nonlinear. This nonlinearity is due to ''dielectric breakdown'' in the solvent chain and the formation of a charge-separated ground state. (Formation of the charge-separated state is analogous to a transition to a cyanine electronic structure, although in the current calculations, the geometry is fixed at the polyene structure.) This transition occurs when the energy required to form a charge-separated solvent state is offset by the enhanced Coulomb interaction with the solute charge distribution. There is some critical value for the magnitude of the solute charge distribution, ζ of Fig. 5, at which this occurs. Since the Coulomb interaction energy between the solute and the charge-separated solvent initially increases with solvent chain length, charge separation occurs more easily, i.e., at smaller values of ζ, on long solvent chains. The squares in Fig. 5 show the solvation energy of the charge distribution corresponding to a hole on the first unit cell and an electron on the ninth unit cell of a 9 unit cell solute, multiplied by ζ. With this solute charge distribution, charge separation occurs on the solvent chain when $\zeta>0.5$.

The formation of this charge-separated state is not, in itself, of interest to the current study. While highly-localized charge distributions may be able to induce charge separation in a nearby chain, such charge distributions are not a focus of this paper.[40] The basis functions Φ_a and Φ_a^r do describe the polarization induced by localized charges; however, the basis set is used to describe the polarization induced by much more diffuse charge distributions, namely, those arising from a hole or exciton delocalized over a long polyene chain. We will see below that the solvent basis performs best when ζ is chosen such that Φ_a and Φ_a^r are not in the charge-separated regime.

We will test two separate aspects of the solvent basis. The first is the ability of a linear combination of an unpolarized and polarized basis function to describe the polarization induced by a charge distribution with identical spatial distribution but different magnitude. Consider the polarization induced by a point charge located at the center of the solute chain in Fig. 1. We define Φ_q as the solvent wave function in the presence of a point charge of magnitude q, calculated from Eq. (10). A basis for the polarization induced by an arbitrary point charge, q', is then constructed from the unpolarized solvent Φ_0 and the polarized solvent Φ_q,

$$\Psi^{\text{solvent}}=c_0\Phi_0+c_1\Phi_q. \tag{13}$$

The linear variational coefficients, c_0 and c_1, are determined from the lowest-energy eigenvector of the Hamiltonian, H' of Eq. (10), in the basis $[\Phi_0,\Phi_q]$. The matrix elements are determined as described in the Appendix. Figure 6 compares the solvation energy obtained from the above basis set to that obtained from explicit solutions of H'. Since the energy of the polarized solvent is calculated variationally, a better basis set gives a lower energy for the polarized solvent and thus a larger solvation energy. The basis $[\Phi_0,\Phi_{0.2}]$ gives the solvation energy of a charge with magnitude between $q'=0.0$ and 0.4 with an accuracy of better than 0.75%, equivalent to the magnitude of the nonlinearity in the exact response over this range. Similarly, the basis $[\Phi_0,\Phi_{0.4}]$ gives the solvation energy of a charge with magnitude between 0.0 and 0.8 to an accuracy of better than 4%, which is once again equivalent to the magnitude of the nonlinearity in the exact response over this range. A unit point charge is sufficient to induce charge-separation in the solvent, as indicated by the rapid increase in the exact solvation energy for $q'>0.9$. Φ_1 then describes a charge-separated solvent, and Fig. 6 indicates

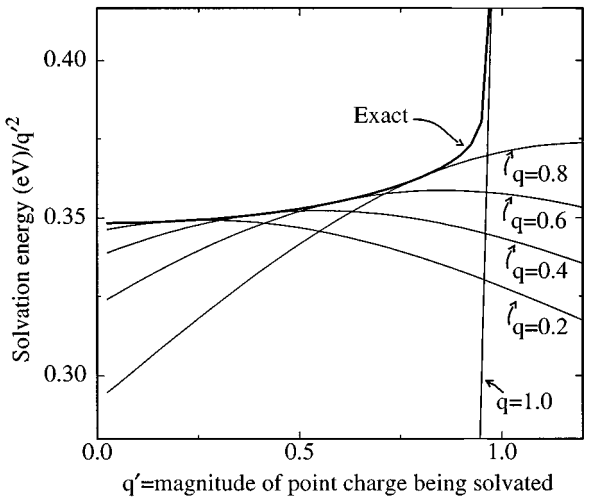

FIG. 6. The solvation energy of a point charge with magnitude q' located at the center of the solute chain in Fig. 1. The ''exact'' result is obtained from direct solution of Eq. (10). Also shown are results obtained with a basis set consisting of two basis functions; the unpolarized solvent and the solvent as polarized by a charge with magnitude q [see Eq. (13)]. Since the energy of the polarized solvent is calculated variationally, a better basis set will give a larger solvation energy.

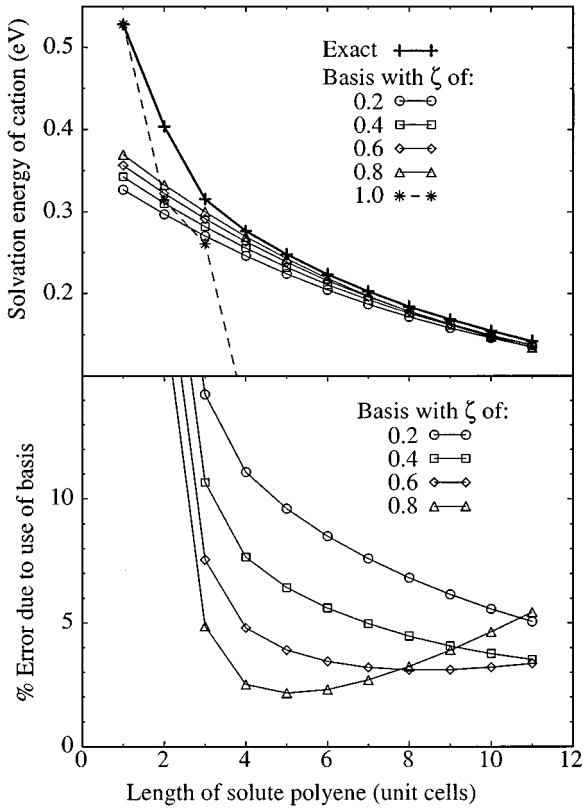

FIG. 7. The upper panel shows the solvation energy of the static charge distribution corresponding to positively charged polyenes of various lengths. The ''exact'' result is obtained from direct solution of Eq. (10). Also shown are results obtained with the basis set of Eq. (11). The lower panel shows the disagreement between the basis set results and the ''exact'' results. Since the energy of the polarized solvent is calculated variationally, a better basis set will give a larger solvation energy.

that the basis $[\Phi_0,\Phi_1]$ does not provide a good description of the solvent polarization in the noncharge-separated regime.

Next, we test the ability of the basis of Eq. (11), constructed from the polarization induced by localized charge distributions, to describe the polarization induced by a diffuse charge distribution. Consider the delocalized charge distribution of an isolated cationic polyene, as described by Eq. (8). The exact solvation energy of this charge distribution by a solvent chain with 40 unit cells, obtained from direct solution of H' in Eq. (10), is shown as the thick solid line in the upper panel of Fig. 7. Note that the localized charge distribution of a solute cation with 1 or 2 unit cells induces charge separation in the solvent chain and this leads to an anomalously large solvation energy. Also shown in Fig. 7 are the solvation energies obtained from diagonalizing H' of Eq. (10) in the basis of Eq. (11). With $\zeta=1$, the solvent basis functions Φ_a are in the charge-separated regime (see Fig. 5), and the basis gives a poor description of the polarization induced by the diffuse charge distribution of a polyene cation with three or more unit cells. With $\zeta=0.2$ and a solute chain length of greater than three unit cells, the error introduced by using the basis of Eq. (11) is less than 10%. For $\zeta=0.6$, the error drops to under 5%. Note also that the use of the solvent basis suppresses charge-separation in the solvent chain, as evidenced by the absence of an enhanced solvation energy at short chain lengths in Fig. 7.

B. Relevant time scales

A simple approach to the inclusion of Coulomb screening in solid-state calculations is to adjust the single-chain electron–electron interaction potential, $U(r)$ of Eq. (3). Rather substantial changes in $U(r)$ are needed to obtain agreement with solid-state experiments. For instance, to obtain an exciton binding energy of 0.5 eV in polydiacetylene, Abe and co-workers[19] lowered the Hubbard parameter, U, from 11 eV to about 5 eV and used a dielectric constant of greater than 5 for the long-range Coulomb interaction. If we assume that the Ohno parametrization, Eq. (3) with $U=11.13$ eV, is appropriate for isolated molecules and that interactions between chains can be incorporated by modifying $U(r)$, a number of physically unreasonable predictions result. For instance, since the ground state energy includes Coulomb interactions between all pairs of electrons, lowering U by a few eV lowers the ground state energy by many eV's per π-electron. This reduction in ground-state energy corresponds to an unphysically large solid-state cohesion energy. Solid-state cohesion arises from dispersion forces and interactions between permanent moments, neither of which is well modeled by changing $U(r)$.

Including Coulomb screening from adjacent chains by modifying $U(r)$ could be rationalized if the motion of electrons on the solvent chains was much faster than that on the solute chain. If this were true, then the polarization of the solvent chains would be set by the instantaneous charge distribution on the solute, thereby screening the electron–electron interaction. However, it is unlikely that such a separation of time scales is valid.

Rather than modify electron–electron interactions, the methods developed below consider how interchain interactions modify the electron–hole interactions present in the excited states. In this case, the relevant time scales are those of the solvent polarization as compared to electron–hole motion. The time scale of the solvent polarization is inversely proportional to the optical gap of about 2 eV. The time scale for electron–hole motion in the exciton is inversely proportional to the exciton binding energy. (A nonstationary state prepared with a dipole moment pointing to the left will oscillate to the right on this time scale.) When the exciton binding energy is only a few percent of the band gap, as in many inorganic semiconductors,[41] the electron–hole motion is orders of magnitude slower than the solvent polarization. In such systems, the polarization of the surroundings can follow the motion of the electron and hole and thus a screened electron–hole interaction potential is used in Wannier exciton theory.[41] But in polymers, the exciton binding energies may be greater than 2.5 eV for an isolated chain (Sec. III) and 0.5 eV or larger in the solid state.[3–5,13] A separation of time scales is then not apparent. (The time scale of electron–hole motion in the $1\,^1B_u$ state of polyacetylene is set by the exciton binding energy on an undistorted chain. That photoexcitation leads to charged soliton production[6–8] does not imply this binding energy is zero, but only that it is less than the energy to be gained by charged soliton production, i.e., it must be less than twice the binding energy of a charged soliton. The soliton binding energy has been estimated as 0.15 eV from experiment.[8] In Sec. III, the MNDO energy predicted for formation of a free electron–hole pair on an isolated chain is about 6.2 eV if soliton formation is ignored, and about 4.7 eV if soliton formation is included, implying a large soliton binding energy of about 0.75 eV.)

A model that includes the time scale of both the electron–hole motion and the dielectric response is developed in Sec. IV E; but first, we consider two limiting cases.

C. Simplified reaction-field model

The reaction-field model assumes the dielectric response of the solvent is much slower than the charge fluctuations arising from electron–hole motion on the solute. In the implementation used here, the electron and hole on the solute are first delocalized as in Eqs. (7) and (8), and the averaged charge distribution is then solvated. This differs from the self-consistent reaction-field (SCRF) model,[42,43] which allows interaction with the solvent to alter the solute charge distribution. Since the systems studied here do not have a permanent dipole moment, our model should not differ significantly from the SCRF model. An important exception is when solvation effects are sufficiently strong that the SCRF model favors symmetry-breaking on the solute chain. For instance, in the case of a charged polyene, the SCRF model may favor the localization of charge on some portion of the chain. This charge localization is not allowed in the reaction-field model used here, which assumes the solute charge distribution is that of the isolated solute polyene.

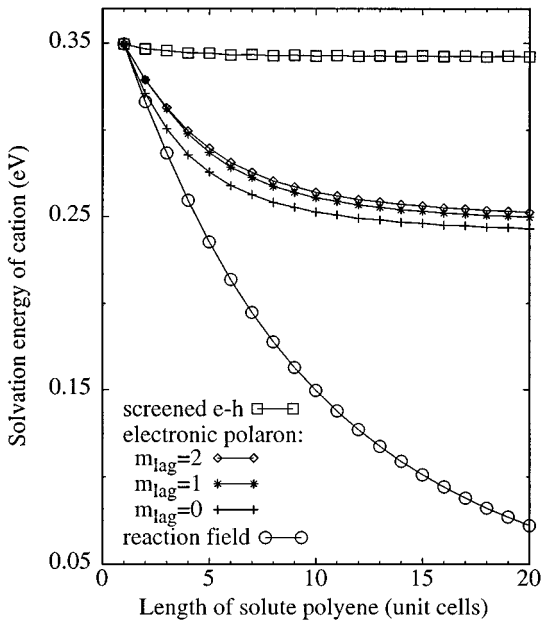

FIG. 8. Solvation energy of a polyene cation due to interaction with a solvent chain with 40 unit cells. The reaction-field, screened $e-h$ and electronic–polaron models are described in Secs. IV C, IV D, and IV E, respectively. All solvation energies are calculated using the solvent basis of Eq. (11), constructed using a scaling factor, $\zeta=0.5$.

The solvation energy is calculated by diagonalizing H' of Eq. (10) in the basis set of Eq. (11). The basis set is constructed with $\zeta=0.5$. (Results for other ζ are shown in Fig. 7.) As discussed at the end of Sec. IV A, the use of the basis suppresses the tendency of a localized charge distribution, such as that of a short polyene cation, to induced charge separation in the solvent chain.

The solvation energies due to interaction with a solvent chain with 40 unit cells are shown as the circles in Figs. 8 and 9. The exciton state, Fig. 9, has no solvation energy in this model since the expectation values, $\langle\hat{\rho}_i\rangle$ of Eq (10), are all zero. These results are discussed further in Sec. V.

D. Screened electron–hole interaction model

This limit is that of Wannier exciton theory,[41] where the dielectric response of the solvent is assumed to be much faster than the charge fluctuations arising from electron–hole motion on the solute. The solvent polarization is then set by the instantaneous position of the electron and hole, leading to dielectric screening of the electron–hole interaction. This model is implemented by starting with the matrix representation of the solute Hamiltonian, H^{sol} of Eq. (2), in the solute basis, ψ_a or ψ_a' of Eqs. (8) and (7). The solvation energy of the charge distributions corresponding to ψ_a or ψ_a' are then calculated using the basis sets of Eqs. (11) or (12), and added to the diagonal of the Hamiltonian matrix. The resulting matrix is then diagonalized. Note that, as discussed at the end of Sec. IV A, the use of the basis set suppresses the tendency of the localized charge distribution of ψ_a or ψ_a' to induce charge separation in the solvent. The calculated solvation energies are shown as the squares in Figs. 8 and 9.

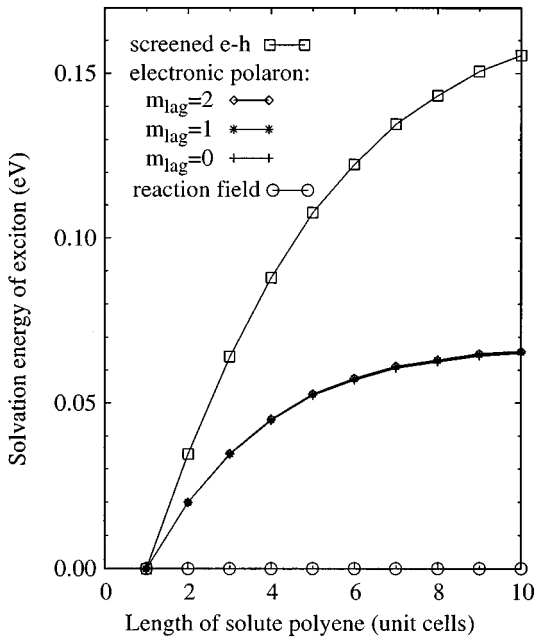

FIG. 9. Solvation energy of the exciton state, due to interaction with a solvent chain with 40 unit cells. All solvation energies are calculated using the solvent basis of Eq. (12) with $\zeta=0.5$. Notation is as in Fig. 8.

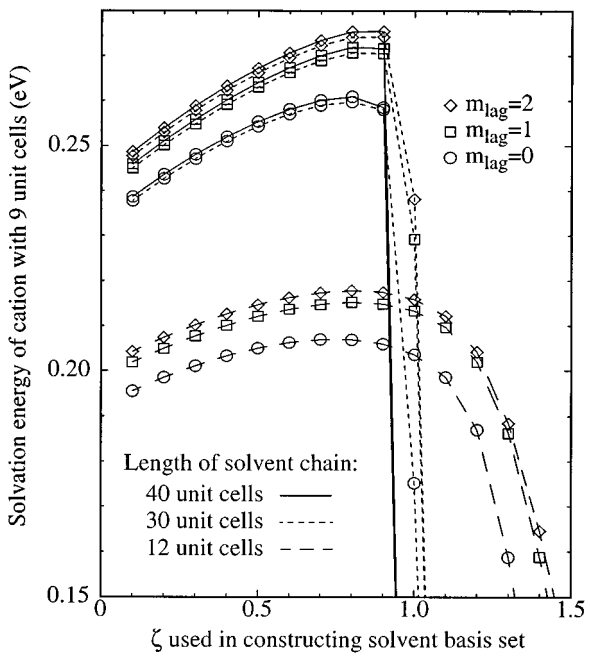

FIG. 10. The solvation energy of a polyene cation with 9 unit cells, calculated using the electronic–polaron model of Sec. IV E. The calculation uses the basis set of Eq. (11), with various values for the scaling parameter ζ. Since the energy of the polarized solvent is calculated variationally, a better basis set will give a larger solvation energy. Comparison with Fig. 5 shows that the basis fails when ζ is such that the basis functions, Φ_a, are charge separated.

E. Electronic–polaron model

In this model, the Hamiltonian of Eq. (1) is diagonalized in a direct-product basis of solute and solvent functions.[44] The solute basis functions are the ψ_a and ψ_a^r of Eqs. (8) and (7). The solvent basis functions are the Φ_a and Φ_a^r of Eqs. (11) and (12). Since the full Hamiltonian is used and the matrix elements are evaluated exactly (see the Appendix), no assumptions are made about the relative time scale of electron–hole motion as compared to solvent polarization.

For the exciton calculation, the size of the complete direct-product basis scales as N^4, N being the number of unit cells on the solute. To avoid this rapid increase in the size of the basis with solute chain length, the following variational form is used for the combined solute–solvent wave function:[45]

$$\Psi=\sum_{a,r}\psi_a^r\left(d_a^r\Phi_0+\sum_{a',r'}c_{a,a'}^{r,r'}\Phi_{a'}^{r'}\right)\left\{\begin{array}{l}|a'-a|\leqslant m_{\mathrm{lag}}\\ |r'-r|\leqslant m_{\mathrm{lag}}\end{array}\right. . \tag{14}$$

A similar basis may be constructed for the cation. As m_{lag} is increased, this basis approaches the full direct-product basis. When $m_{\mathrm{lag}}=0$, each solute function ψ_a^r is paired with the corresponding solvent polarization Φ_a^r; the spatial distribution of the solvent polarization is thereby constrained to follow the motion of the electron and hole on the solute, and the variational procedure adjusts only the magnitude of the polarization by changing the ratio of the c and d coefficients. With $m_{\mathrm{lag}}>0$, the solvent polarization may lag behind the motion of the electron and hole, and the variational procedure has more flexibility in determining the spatial distribution of the polarization.

Figures 10 and 11 show the solvation energy as a func-

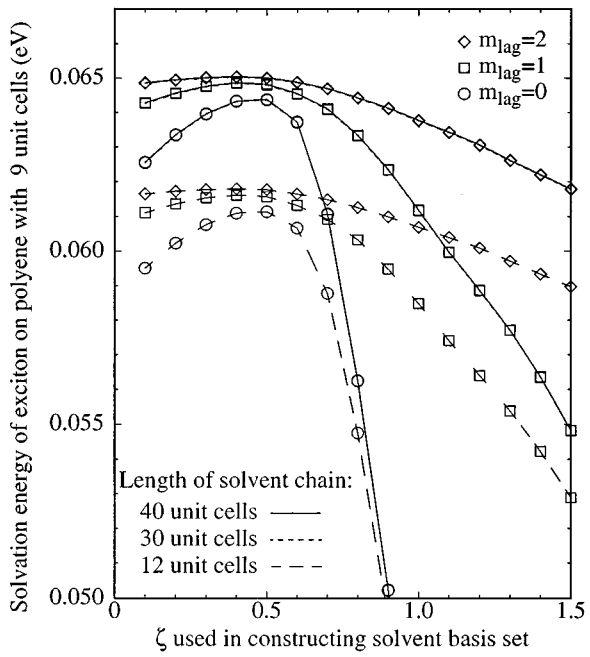

FIG. 11. The solvation energy of the exciton state of a polyene with 9 unit cells, calculated using the electronic–polaron model of Sec. IV E. The calculation uses the basis set of Eq. (12), with various values for the scaling parameter ζ. Since the energy of the polarized solvent is calculated variationally, a better basis set will give a larger solvation energy. Comparison with Fig. 5 shows that more rapid convergence with m_{lag} is obtained when ζ is such that the basis functions Φ_a^r are not charge separated.

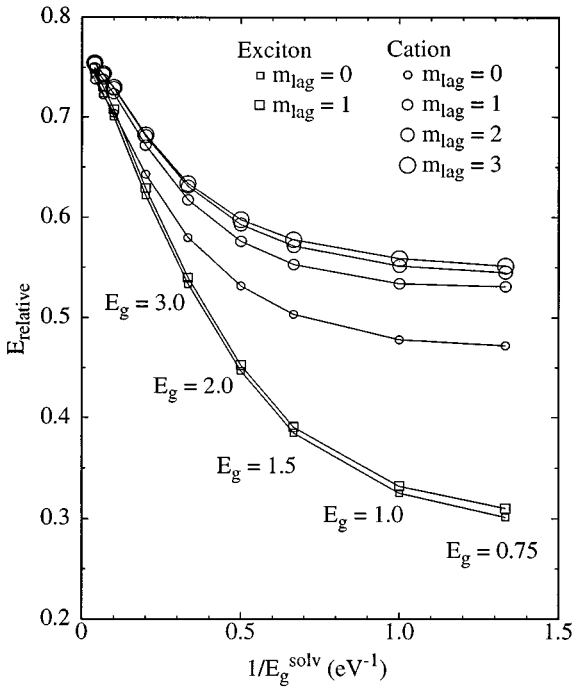

FIG. 12. Comparison of the solvation energies predicted by various electron–hole screening models, as a function of the band gap of the solvent. The solute polyene has 9 unit cells, and the solvent polyene has 40 unit cells. The plotted quantity, E_{relative} of Eq. (15), is 1 when the electronic–polaron model agrees with the screened electron–hole potential model, as is expected when the band gap is large and the solvent polarization is fast. E_{relative} equals 0 when the electronic–polaron model agrees with the reaction-field model, as is expected when the band gap is small and the solvent polarization is slow. The solvent basis is constructed using a scaling factor $\zeta=0.3$.

tion of the scaling factor, ζ, used in constructing the solvent basis. The solute chain has 9 unit cells and the solvent chain has 12, 30 or 40 unit cells. The calculated solvation energy is relatively insensitive to the value of ζ, provided ζ is sufficiently small that the basis functions Φ_a or Φ_a^r are not in the charge-separated regime. Figure 5 shows that charge separation in Φ_a of a 40-unit-cell solvent chain occurs when $\zeta>0.9$, and Fig. 10 shows that above this point, the basis gives a poor description of the solvent polarization. (The procedure is variational in the sense that a better basis set will give a larger solvation energy.) Figure 5 shows that charge separation in Φ_a^r of a 40-unit-cell solvent chain occurs when $\zeta>0.6$, and Fig. 11 shows that this leads to slower convergence with respect to m_{lag}.

Figures 10 and 11 also indicate that the solvation energy is saturated by a solvent chain length of 40 unit cells.

The dependence of the solvation energy on solute chain length is shown in Figs. 8 and 9. The scaling factor, ζ, is fixed at 0.5. The solvation energies from the electronic–polaron model are intermediate between those of the screened electron–hole interaction model and the reaction-field model. This indicates that the time scale for electron–hole motion is comparable to that of the solvent polarization and a separation of time scales is not valid.

Changing the optical gap of the solvent, E_g^{solv} of Eq. (5), changes the time scale of the solvent polarization. Figure 12 shows the solvation energy for a 9 unit cell solute and a 40 unit cell solvent, as a function of the optical gap, E_g^{solv}. The quantity shown is

$$E_{\text{relative}}=\frac{E_{\text{electronic-polaron}}-E_{\text{reaction-field}}}{E_{\text{screened } e-h}-E_{\text{reaction-field}}}, \tag{15}$$

where $E_{\text{electronic-polaron}}$, $E_{\text{reaction-field}}$, and $E_{\text{screened } e-h}$ are the solvation energies obtained from the electronic–polaron, reaction-field, and screened electron–hole interaction models, respectively. When $E_{\text{relative}}=1$, the electronic–polaron model agrees with the screened electron–hole interaction model, and when $E_{\text{relative}}=0$, the electronic–polaron model agrees with the reaction-field model. Since charge separation occurs more easily when the solvent band gap is reduced, a scaling factor of $\zeta=0.3$ is used to insure that the solvent basis functions are not in the charge-separated regime.

V. DISCUSSION

This paper considers separately, the exciton binding energy of a hypothetical isolated chain of polyacetylene, and the effects of interchain interactions on this binding energy. Figures 2–4 use semiempirical quantum chemistry to predict the exciton binding energy of an isolated chain. Since the predictions agree with experiments on short chains, this approach may be viewed as using semiempirical Hartree–Fock theory to extrapolate from molecular data to the polymeric limit. The energy predicted for formation of a free electron–hole pair on an isolated chain of polyacetylene is 6.2 eV if soliton formation is ignored, and about 4.7 eV if soliton formation is included. This is much larger than the observed threshold for charged soliton production in polyacetylene, which is near the optical gap of about 1.8 eV.[6–8]

Interactions with adjacent chains lower the exciton binding energy since the solvation energy of the free electron–hole pair is larger than that of the exciton. The solvation energies, calculated using a number of different models, are shown in Figs. 8 and 9. The solvent chain length is 40 unit cells, sufficient to saturate the calculated solvation energies (see Figs. 10 and 11). Due to particle–hole symmetry in Eq. (1), the solvation energy of a polyene anion is equal to that of the cation, and the solvation energy of a free electron–hole pair is twice that of the cation shown in Fig. 8.

The simplified reaction-field model of Sec. IV C assumes the solvent polarization is much slower than electron–hole motion on the solute. The solvent polarization is then set by the *averaged* charge distribution of the solute. Within this model, the exciton state is nonpolar and has zero solvation energy (Fig. 9). For the cation, as the solute chain length is increased, the solute charge distribution becomes increasingly diffuse and the solvation energy tends toward zero (Fig. 8). Soliton formation will localize the solute charge distribution and lead to a finite solvation energy in the long-chain limit. Given an estimated soliton size[46,47] of 14 unit cells,[48,49] a rough estimate for the solvation energy from this model is that of an undistorted polyene cation with 14 unit cells, about 0.1 eV in Fig. 8.

At the opposite extreme is the screened electron–hole interaction model of Sec. IV D, which assumes the solvent polarization is much faster than electron–hole motion. The solvent polarization is then set by the *instantaneous* position of the electron and hole, thus screening the electron–hole interaction. In this model, the solvation energy of the exciton is about 0.16 eV (Fig. 9), and that of a well separated electron and hole is twice that of the cation, about 0.68 eV (Fig. 8). The exciton binding energy is then reduced by 0.52 eV.

The electronic–polaron model of Sec. IV E makes no assumptions about the relative time scale of electron–hole motion vs solvent polarization. Figures 8 and 9 show that the predicted solvation energies lie between those of the reaction-field and screened electron–hole interaction models. This can be understood as follows. Formation of a polarization cloud around the electron and hole leads to a favorable electrostatic interaction between the solute and solvent chains; however, the resulting increase in the effective mass of the electron and hole lowers the delocalization energy. The electronic–polaron model includes these changes in effective mass, since it calculates the matrix elements of the full Hamiltonian, Eq. (1), between the basis functions of Eq. (14). However, the increase in effective mass is ignored by the screened electron–hole interaction model, which modifies only the Coulomb interaction between the electron and hole. The screened electron–hole interaction model thereby overestimates the solvation energy of the exciton by 130% and of the cation by 35%, relative to the electronic–polaron model. Since the overestimation is larger for the exciton, and the screened electron–hole interaction model is valid for slow electron–hole motion, this suggests that electron–hole motion is faster in the exciton than in the cation or anion.

The electronic–polaron model gives a solvation energy of about 0.50 eV for a free electron–hole pair (twice that of the cation in Fig. 8) and 0.07 eV for the exciton (Fig. 9). The predicted reduction of the exciton binding energy is then about 0.43 eV, a relatively large number for interaction with a single chain.

The time scale of the solvent polarization is set by the optical gap of the solvent chain. Figure 12 shows the relative solvation energies for a range of solvent optical gaps. The quantity shown, E_{relative} of Eq. (15), is 1 when the electronic–polaron model agrees with the screened electron–hole interaction model and 0 when the electronic–polaron model agrees with the reaction-field model. The results of Fig. 12 show the expected trend. For large solvent optical gaps, corresponding to a fast dielectric response, the solvation energy tends towards the screened electron–hole interaction model. For small solvent optical gaps, corresponding to slow dielectric response, the solvation energy tends towards the reaction-field model. However, it is not clear why E_{relative} does not identically approach these limits. In the screened electron–hole interaction model, the size of the electron and hole is set by the localized Hartree–Fock orbitals obtained from calculations on an isolated chain (see Sec. III). That E_{relative} does not identically approach one in the large band-gap limit may indicate that the localized Hartree–Fock orbitals are not the optimal choice for the form of the electron and hole in the large band-gap limit. In the small band-gap limit, E_{relative} for the exciton approaches something near zero; however, E_{relative} for the cation-approaches 0.5. This may indicate that the charge on the cation self-traps, forming an electronic polaron with a bandwidth that goes to zero in the limit of an infinitely slow dielectric response. As discussed in Sec. IV C, the reaction field model used here assumes the solute charge distribution is that of the isolated solute, and thus does not allow the solvent to induce charge localization on the solute.

To address the solid-state exciton binding energy, we are working on the following extensions to the model. First, the number of solvent chains must be increased to allow extrapolation to the solid-state limit. On-chain polarization effects also need to be included. In the electronic–polaron model introduced here, the electron and hole are dressed by the polarization of the solvent chain. In addition, the electron and hole may be dressed by on-chain polarization, which is ignored in Hartree–Fock and S-CI theory. Suhai[37,38] and Liegener[39] find that on-chain polarization has a large effect on the exciton binding energies calculated from *ab initio* theory. In a semiempirical Hartree–Fock approach, the parameterization to small molecules may partially include such on-chain polarization effects. However, if the effects of on-chain polarization are chain-length dependent, the use of semiempirical Hartree–Fock theory to extrapolate from short to long chains, as in Figs. 2–4, may not be valid. Finally, sigma electrons should be included in the solvent chain. Addition of sigma electrons to the solvent is not expected to greatly alter the polarizability along the chain, however, it will likely have large effects on the polarization perpendicular to the polymer axis. This is especially true for the polarizability perpendicular to the plane of the polymer, which is zero in a pi-electron model. (This component of the polarizability does not contribute to the solvation energy in the geometry of Fig. 1.)

The electronic–polaron model presented here finds that interaction with a single chain lowers the exciton binding energy by 0.43 eV. Given this large reduction from interaction with a single chain, these calculations strongly suggest that interchain interactions play an important role in establishing the exciton binding energy. The calculations presented here also strongly suggest that interchain interactions are not well modeled by simply reparametrizing a single chain Hamiltonian to solid-state data. By developing an explicit model of Coulomb screening, we hope to achieve a more realistic model of the photophysics of conjugated polymers, with better transferability of parameters between polymer systems, and with the ability to utilize detailed information available from both experimental studies and *ab initio* calculations on molecular systems to make predictions for solid state properties.

ACKNOWLEDGMENT

This work was supported by the National Science Foundation (Grant No. CHE-9530148).

APPENDIX: HAMILTONIAN MATRIX ELEMENTS

The matrix elements of the Hamiltonian, Eq. (1), between the basis functions of Eq. (14) are

$$\begin{aligned}\langle \psi_b^s \Phi_{b'}^{s'} | H | \psi_a^r \Phi_{a'}^{r'} \rangle &= \langle \psi_b^s | H^{\mathrm{sol}} | \psi_a^r \rangle \langle \Phi_{b'}^{s'} | \Phi_{a'}^{r'} \rangle \\ &+ \delta_{a,b}\delta_{r,s} \langle \Phi_{b'}^{s'} | H^{\mathrm{solv}} | \Phi_{a'}^{r'} \rangle \\ &+ \sum_{i,I} U(r_{I,i}) \langle \Phi_{b'}^{s'} | \hat{\rho}_I | \Phi_{a'}^{r'} \rangle \\ &\times \langle \psi_b^s | \hat{\rho}_i | \psi_a^r \rangle . \end{aligned} \tag{A1}$$

The matrix elements between solute functions are the standard matrix elements of CI theory.[28] The matrix elements between solvent functions are calculated as follows.

Consider two single Slater determinant wave functions, such as $\Phi_{b'}^{s'}$ and $\Phi_{a'}^{r'}$ of Eq. (A1), that describe the solvent in the presence of two different solute charge distributions

$$\Phi_{b'}^{s'} = \overline{a_1^\dagger a_2^\dagger} \ldots |0\rangle; \quad \Phi_{a'}^{r'} = a_1^\dagger a_2^\dagger \ldots |0\rangle, \tag{A2}$$

where $a_i^\dagger$ creates an electron in spin–orbital ϕ_i of $\Phi_{a'}^{r'}$, and $\overline{a_i^\dagger}$ creates an electron in spin–orbital $\overline{\phi_i}$ of $\Phi_{b'}^{s'}$.

The overlap between the wave functions is

$$\langle \Phi_{b'}^{s'} | \Phi_{a'}^{r'} \rangle = |S^{\mathrm{occ}}|, \tag{A3}$$

where S^{occ} is a matrix holding the overlaps between the occupied spin–orbitals,

$$S_{i,j}^{\mathrm{occ}} = \langle \overline{\phi_i} | \phi_j \rangle; \quad i,j = 1 \ldots N_{\mathrm{occ}}, \tag{A4}$$

N_{occ} is the number of occupied spin–orbitals in $\Phi_{b'}^{s'}$ and $\Phi_{a'}^{r'}$, and $|M|$ refers to the determinant of the matrix M.

The matrix elements of a one-electron operator can be obtained by first expanding the operator in the spin–orbital basis of $\Phi_{a'}^{r'}$,

$$\hat{O} = \sum_{i,j} O_{i,j} a_i^\dagger a_j , \tag{A5}$$

where $O_{i,j} = \langle \phi_i | \hat{O} | \phi_j \rangle$. The matrix element of the operator may now be written

$$\langle \Phi_{b'}^{s'} | \hat{O} | \Phi_{a'}^{r'} \rangle = |S^{\mathrm{occ}}| \sum_a O_{a,a} + \sum_{a,r} O_{r,a} |S_a^r|, \tag{A6}$$

where a is summed over the occupied spin–orbitals of $\Phi_{a'}^{r'}$ and r is summed over the unoccupied spin–orbitals of $\Phi_{a'}^{r'}$. S_a^r is a matrix obtained from S^{occ} by replacing the ath column of S_{occ} as follows:

$$(S_a^r)_{i,j} = \begin{cases} S_{i,j}^{\mathrm{occ}} & (j \neq a) \\ \langle \overline{\phi_i} | \phi_r \rangle & (j = a) \end{cases}. \tag{A7}$$

An efficient computational evaluation of Eq. (A6) may be achieved by writing $|S^{\mathrm{occ}}|$ as

$$|S^{\mathrm{occ}}| = \sum_i S_{i,j}^{\mathrm{occ}} C_{i,j} , \tag{A8}$$

where C is the matrix of cofactors of S^{occ}. The determinant of S_a^r can then be obtained from,

$$|S_a^r| = \sum_i \langle \overline{\phi_i} | \phi_r \rangle C_{i,a} . \tag{A9}$$

The computationally expensive step of evaluating the cofactor matrix, C, need be done only once for each set of functions, $\Phi_{a'}^{r'}$ and $\Phi_{b'}^{s'}$. We could not find a similar computational simplification for a two-electron operator, and this is our primary motivation for using the Hückel Hamiltonian, Eq. (4), to describe the solvent.

Assuming $\Phi_{a'}^{r'}$ and $\Phi_{b'}^{s'}$ contain doubly occupied spatial orbitals leads to further simplification, and Eq. (A6) becomes

$$\langle \Phi_{b'}^{s'} | \hat{O} | \Phi_{a'}^{r'} \rangle = 2|S^{\mathrm{occ}}|^2 \sum_a O_{a,a} + 2|S^{\mathrm{occ}}| \sum_{a,r} O_{r,a} |S_a^r|, \tag{A10}$$

where the matrices and summations are as above, but with all indices referring to spatial rather than spin–orbitals.

[1] G. Gustafsson, Y. Cao, G. M. Treacy, F. Klavetter, N. Colaneri, and A. J. Heeger, Nature **357**, 477 (1992).
[2] J. H. Burroughes, D. D. C. Bradley, A. R. Brown, R. N. Marks, K. Mackay, R. H. Friend, P. L. Burns, and A. B. Holmes, Nature **347**, 539 (1990).
[3] K. Lochner, H. Bassler, B. Tieke, and G. Wegner, Phys. Status Solidi B **88**, 653 (1978).
[4] L. Sebastian and G. Weiser, Phys. Rev. Lett. **46**, 1156 (1981).
[5] L. Sebastian and G. Weiser, Chem. Phys. **62**, 447 (1981).
[6] G. B. Blanchet, C. R. Fincher, and A. J. Heeger, Phys. Rev. Lett. **51**, 2132 (1983).
[7] L. Rothberg, T. M. Jedju, P. D. Townsend, S. Etemad, and G. L. Baker, Phys. Rev. Lett. **65**, 100 (1990).
[8] Z. V. Vardeny, Prog. Theor. Phys. Suppl. **113**, 97 (1993).
[9] K. Pakbaz, C. H. Lee, A. J. Heeger, T. W. Hagler, and D. McBranch, Synth. Met. **64**, 295 (1994).
[10] I. H. Campbell, T. W. Hagler, D. L. Smith, and J. P. Ferraris, Phys. Rev. Lett. **76**, 1900 (1996).
[11] R. N. Marks, J. J. M. Halls, D. D. C. Bradley, R. H. Friend, and A. B. Holmes, J. Phys. Condens. Matter **6**, 1379 (1994).
[12] M. Deussen, M. Scheidler, and H. Bassler, Synth. Met. **73**, 123 (1995).
[13] J. M. Leng, S. Jeglinski, X. Wei, R. E. Benner, Z. V. Vardeny, F. Guo, and S. Mazumdar, Phys. Rev. Lett. **72**, 156 (1994).
[14] M. Chandross, S. Mazumdar, S. Jeglinski, X. Wei, Z. V. Vardeny, E. W. Kwock, and T. M. Miller, Phys. Rev. B **50**, 14 702 (1994).
[15] P. G. da Costa and E. M. Conwell, Phys. Rev. B **48**, 1993 (1993).
[16] Z. Shuai, J. L. Bredas, and W. P. Su, Chem. Phys. Lett. **228**, 301 (1994).
[17] T. Hasegawa, Y. Iwasa, H. Sunamura, T. Koda, Y. Tokura, H. Tachibana, M. Matsumoto, and S. Abe, Phys. Rev. Lett. **69**, 668 (1992).
[18] S. Abe, J. Yu, and W. P. Su, Phys. Rev. B **45**, 8264 (1992).
[19] S. Abe, M. Schrieber, W. P. Su, and J. Yu, J. Lumin. **53**, 519 (1992).
[20] S. Mazumdar and F. Guo, J. Chem. Phys. **100**, 1665 (1994).
[21] I. Ohmine, M. Karplus, and K. Schulten, J. Chem. Phys. **68**, 2298 (1978).
[22] J. Ridley and M. Zerner, Theor. Chim. Acta **32**, 111 (1973).
[23] M. J. S. Dewar and W. Thiel, J. Am. Chem. Soc. **99**, 4899 (1977).
[24] Z. G. Soos, G. W. Hayden, P. C. M. McWilliams, and S. Etemad, J. Chem. Phys. **93**, 7439 (1990).
[25] P. C. M. McWilliams and Z. G. Soos, J. Chem. Phys. **95**, 2127 (1991).
[26] S. Lias, J. Bartmess, J. Liebman, J. Holmes, R. Devin, and W. G. Mallard, J. Phys. Chem. Ref. Data **17**, Suppl. 1, 1 (1988).
[27] J. Hinze and H. H. Jaffe, J. Am. Chem. Soc. **84**, 540 (1962).
[28] A. Szabo and N. Ostlund, *Modern Quantum Chemistry* (McGraw–Hill, New York, 1989).
[29] M. Kertesz, Chem. Phys. **44**, 349 (1979).
[30] D. Yaron and R. Silbey, Phys. Rev. B **45**, 11 655 (1992).
[31] D. Yaron, Mol. Cryst. Liquid Cryst. **256**, 631 (1994).

[32] M. J. S. Dewar, E. G. Zoebisch, E. F. Healy, and J. J. P. Stewart, J. Am. Chem. Soc. **107**, 3902 (1985).
[33] P. Tavan and K. Schulten, Phys. Rev. B **36**, 4337 (1987).
[34] B. E. Kohler, C. Spangler, and C. Westerfield, J. Chem. Phys. **89**, 5422 (1988).
[35] J. J. P. Stewart, QCPE #455 (The calculations presented here used version 6.00 of the MOPAC program).
[36] J. Cornil, D. Beljonne, R. H. Friend, and J. L. Bredas, Chem. Phys. Lett. **223**, 82 (1994). (The band edge of S-CI theory occurs at the Hartree–Fock gap, which in Fig. 3 occurs at about 6 eV. Table I lists the energy of the lowest state as 3.24 eV, for an exciton binding energy of about 2.75 eV.)
[37] S. Suhai, Phys. Rev. B **27**, 3506 (1983).
[38] S. Suhai, Int. J. Quantum Chem. **29**, 469 (1986).
[39] C.-M. Liegener, J. Chem. Phys. **88**, 6999 (1988).
[40] In fact, to study charge separation, we would need to go beyond a Huckel description of the solvent, since Huckel theory likely underestimates the energy required for charge separation.
[41] R. Knox, *Theory of Excitons*, *Solid State Physics: Supplement 5* (Academic, New York, 1963).
[42] J. Tomasi and M. Persico, Chem. Rev. **94**, 2027 (1994).
[43] M. W. Wong, K. B. Wiberg, and M. Frisch, J. Am. Chem. Soc. **114**, 1645 (1992).
[44] H. J. Kim, R. Bianco, B. J. Gertner, and J. T. Hynes, J. Phys. Chem. **97**, 1723 (1993).
[45] When the electron and hole are on the same unit cell, $a=r$, the solute atoms are uncharged and Φ_a^r is equal to Φ_0. The basis functions $\psi_a^r\Phi_0$ and $\psi_a^r\Phi_a^r$ are then identical and are included only once in the basis.
[46] H. Thomann, L. R. Dalton, M. Grabowski, and T. C. Clarke, Phys. Rev. B **31**, 3141 (1985).
[47] S. Kuroda and H. Shirakawa, Phys. Rev. B **35**, 9380 (1987).
[48] M. Mehring, A. Grupp, P. Hover, and H. Kass, Synth. Met. **28**, D399 (1989).
[49] B. Kirtman, M. Hasan, and D. M. Chipman, J. Chem. Phys. **95**, 7698 (1991).